Biosensors and Bioelectronics 219 (2023) 114836

Contents lists available at ScienceDirect

Biosensors and Bioelectronics

journal homepage: www.elsevier.com/locate/bios

A novel cascade signal amplification strategy integrating CRISPR/Cas13a and branched hybridization chain reaction for ultra-sensitive and specific SERS detection of disease-related nucleic acids

Jingjing Zhang [a], Chunyuan Song [a,c,*], Yunfeng Zhu [a], Hongyu Gan [a], Xinyue Fang [a], Qian Peng [a], Jingrong Xiong [a], Chen Dong [a], Caiqin Han [b,**], Lianhui Wang [a,***]

[a] State Key Laboratory for Organic Electronics and Information Displays, Jiangsu Key Laboratory for Biosensors, Institute of Advanced Materials (IAM), Jiangsu National Synergetic Innovation Center for Advanced Materials (SICAM), Nanjing University of Posts & Telecommunications, Nanjing, 210023, China
[b] Jiangsu Key Laboratory of Advanced Laser Materials and Devices, School of Physics and Electronic Engineering, Jiangsu Normal University, Xuzhou, 22116, China
[c] State Key Laboratory of Applied Optics, Changchun Institute of Optics, Fine Mechanics and Physics, Chinese Academy of Sciences, Changchun, 130033, China

ARTICLE INFO

Keywords:
SERS
CRISPR/Cas13a
Branched hybridization chain reaction
Cascade signal amplification
Nucleic acids

ABSTRACT

The molecular diagnosis of disease by high-sensitively and specifically detecting extremely trace amounts of nucleic acid biomarkers in biological samples is still a great challenge, and the powerful sensing strategy has become an urgent need for basic researches and clinical applications. Herein, a novel one-pot cascade signal amplification strategy (Cas13a-bHCR) integrating CRISPR/Cas13a system (Cas13a) and branched hybridization chain reaction (bHCR) was proposed for ultra-highly sensitive and specific SERS assay of disease-related nucleic acids on SERS-active silver nanorods sensing chips. The Cas13a-bHCR based SERS assay of gastric cancer-related miRNA-106a (miR-106a) can be achieved within 60 min and output significantly enhanced SERS signal due to the multiple signal amplification, which possesses a good linear calibration curve from 10 aM to 1 nM with the limit of detection (LOD) low to 8.55 aM for detecting gastric cancer-related miR-106a in human serum. The Cas13a-bHCR based SERS sensing also shows good specificity, uniformity, repeatability and reliability, and has good practicability for detection of miR-106a in clinical samples, which can provide a potential powerful tool for SERS detection of disease-related nucleic acids and promise brighter prospects in the field of clinical diagnosis of early disease.

1. Introduction

Despite the great success of immunoassay, some deficiencies have gradually emerged, for instance, the selection of target protein-related immunoproteins is very limited and the detection cannot achieve the cyclic amplification of target protein to obtain the higher sensitivity by the signal amplification strategy (Tate and Ward, 2004; Wang et al., 2021; Xu et al., 2021). In recent years, the molecular diagnosis of disease for detecting disease-related nucleic acids becomes a more and more important tool for disease identification, prevention, and treatment (Hui et al., 2021; Nam et al., 2022; Wang et al., 2019; Xu et al., 2018; Zhang et al., 2020). The high-sensitive and specific detection of extremely trace amounts of nucleic acid biomarkers in biological samples is a great challenge, and the excellent/powerful nucleic acids sensing strategy has become an urgent need for basic researches and clinical applications. Aiming to the high-sensitive and reliable detection requirements, a feasible solution is to amplify the trace amounts of nucleic acids. Recently, the real-time polymerase chain reaction (RT-PCR) is considered as a typical amplification strategy utilized in nucleic acid detection by continuous replication of the target nucleic acids under the action of polymerase (Bienko et al., 2013; Markou et al., 2008; Smyrlaki et al., 2020). Moreover, the isothermal amplification technologies, such as

* Corresponding author. State Key Laboratory for Organic Electronics and Information Displays, Jiangsu Key Laboratory for Biosensors, Institute of Advanced Materials (IAM), Jiangsu National Synergetic Innovation Center for Advanced Materials (SICAM), Nanjing University of Posts & Telecommunications, Nanjing, 210023, China.
** Corresponding author.
*** Corresponding author.
E-mail addresses: iamcysong@njupt.edu.cn (C. Song), hancq@jsnu.edu.cn (C. Han), iamlhwang@njupt.edu.cn (L. Wang).

https://doi.org/10.1016/j.bios.2022.114836
Received 4 July 2022; Received in revised form 7 October 2022; Accepted 17 October 2022
Available online 22 October 2022

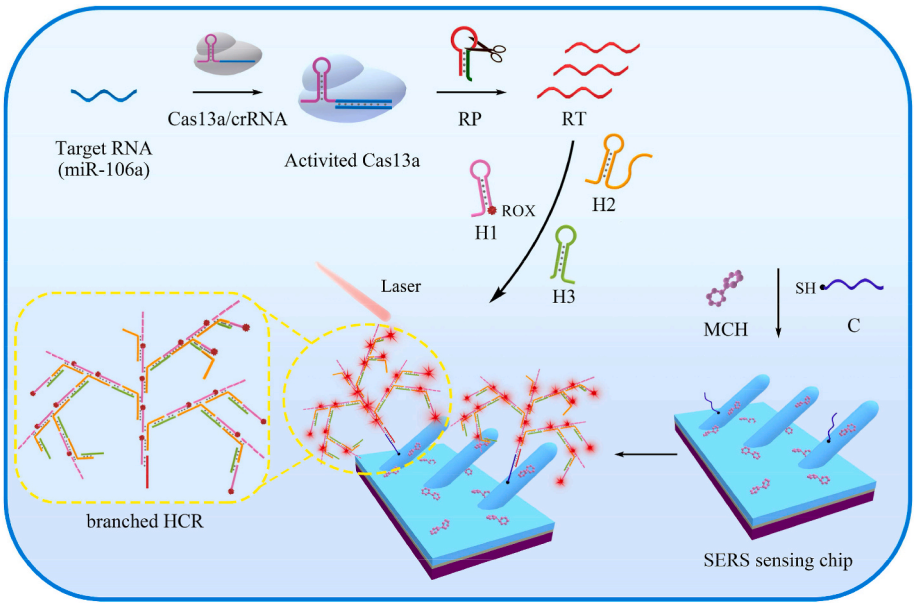

Scheme 1. Schematic illustration of the sensing mechanism of Cas13a-bHCR based cascade signal amplification strategy for SERS sensing disease-related miRNA.

loop-mediated isothermal amplification (LAMP) (Notomi et al., 2000; Tomita et al., 2008) and recombinase polymerase amplification (RPA) (Kong et al., 2019; Rohrman and Richards-Kortum, 2012), have been developed as an attractive alternative to conventional PCR. However, these amplification strategies based on the replication of nucleic acids are limited by the requirements of precise primer design, fine thermal control, complex operations, which make the detections expensive, time consuming, possibly non-specific and vulnerable to the high risk of carry-over contamination caused false positives (Liu et al., 2020; Wang et al., 2011). Therefore, the development of nucleic acid amplification-free strategy, i.e., the signal amplifications without amplifying the target nucleic acid, has great significance in molecular diagnosis, however the strategy that meets the tough requirements of highly sensitive detection of ultra-low analyte remains a big challenge.

The recently discovered clustered regularly interspaced short palindromic repeats (CRISPR) and CRISPR-associated (Cas) protein systems have provided further possibilities in molecular diagnostics (Choi et al., 2021; Gootenberg et al., 2017; Li et al., 2019; Tang et al., 2022; Wang et al., 2020; Wu et al., 2021). It has been confirmed that the CRISPR/Cas13a system has crRNA-guided recognition ability to specific target RNA, followed by the activation of promiscuous ribonuclease (RNase) activity of Cas13a to cleave nonspecifically the rationally designed nucleic acid reporters (Gootenberg et al., 2017; Kellner et al., 2019; Li, H. et al., 2022b; Liu et al., 2017), which is known as a highly specific and universal tool for gene editing. The RNase activity is highly efficient, with at least 10^4 turnovers per target RNA recognized, resulting in four orders of magnitude of signal amplification (East-Seletsky et al., 2016; Gootenberg et al., 2017; Tian et al., 2021). In addition, the hybridization chain reaction (HCR) which can spontaneously hybridize in the presence of a single-stranded target nucleic acid to generate numerous hairpin complexes is known as a simple, robust and efficient tool for enzyme-free isothermal signal amplification without amplifying target nucleic acid to generate obviously enhanced signal with the exemption of a complicated enzyme reaction (Cheng et al., 2021; Gao et al., 2022; Huang et al., 2018; Jiao et al., 2020; Yang et al., 2022). Generally, a single signal amplification is limited by the requirement of both ultra-high specificity and low-abundance sensitivity for liquid biopsy and pathogen detection (Ang and Yung, 2016; Li et al., 2020; Tian et al., 2021; Wang et al., 2018). Therefore, the design of nonlinear hybridization chain reaction (i.e., branched hybridization chain reaction (bHCR)) with improved amplification and a novel cascade signal amplification basing on the CRISPR/Cas13a system and bHCR is expected to achieve high specificity and sensitivity (Gootenberg et al., 2017). Besides the signal amplifications, the development of ultra-sensitive sensing techniques is another direction to achieve high-sensitive biosensing (Zhou et al., 2018), and the way to develop sensing strategies based on more sensitive SERS techniques for replacing traditional fluorescence-based detection methods is promising and effective for trace disease-related nucleic acids (Alvarez-Puebla et al., 2018; Moisoiu et al., 2021; Nie and Emory, 1997; Zhu et al., 2022; Zong et al., 2018). In the previous works (Abell et al., 2011; Driskell et al., 2008; Liu et al., 2010), the silver nanorods (AgNRs) array (AgNRs with about 1000 nm length and 100 nm diameter) shows excellent SERS performance with an enhancement factor (EF) up to 10^9, and provides a uniform and stable response (relative standard deviation (RSD)<10%) across the area of the same substrate and shows good reproducibility (RSD<15%) in different batches of substrates, which can be successfully used to SERS-based high-sensitively detect different biological and chemical agents (Song et al., 2020b; Zhang et al., 2022).

In this work, a novel one-pot cascade signal amplification strategy integrating CRISPR/Cas13a system (Cas13a) and branched hybridization chain reaction (bHCR) was proposed on SERS-active AgNRs array sensing chips for ultra-highly sensitive and specific SERS detection of disease-related nucleic acids. The Cas13a-bHCR based cascade signal amplification strategy includes three components, i.e., a CRISPR/Cas13a system, branched hybridization chain reactions, and SERS sensing chips. Taking the detection of gastric cancer-related miRNA-106a (miR-106a) as an example, the sensing mechanism and feasibility of the Cas13a-bHCR based cascade signal amplification strategy were characterized and the preferable sensing parameters were optimized first. Then, the excellent performance of the cascade signal amplification strategy was investigated by comparing the SERS assays based on the single CRISPR/Cas13a strategy. Finally, the sensing performance of Cas13a-bHCR based SERS strategy on sensitivity, specificity, uniformity, repeatability and practicability were investigated, which indicates that the proposed Cas13a-bHCR based SERS strategy can provide an ultra-sensitive and specific tool for SERS detection of disease-related nucleic acids.

2. Experimental section

2.1. Material and apparatus

The LbuCas13a protein (Cas13a) was purchased from Bio-lifesci (Guangzhou, China). Mercaptohexanol (MCH, 97%) was obtained from Sigma-Aldrich (Shanghai, China). Human serum was purchased from Beijing China Science Chenyu Technology Co., Ltd (Beijing, China). Diethyl pyrocarbonate (DEPC) water was obtained from Sangon Biotechnology Co., Ltd. (Shanghai, China). All the single-stranded DNA (ssDNA) and RNA (ssRNA) listed in Table S1 were purified by high-performance liquid chromatography (HPLC) and synthesized by Sangon Biotechnology Co., Ltd. (Shanghai, China). The ssDNA and ssRNA were treated with DEPC first to avoid the degradation. The hybridizations were performed in reaction buffer (10 mM Tris-HCl, 50 mM KCl, 1.5 mM $MgCl_2$, pH 8.3). Millipore ultrapure water (18.2 MΩ cm) was used to prepare various solutions which were autoclaved to avoid the degradation of RNA. Clinical blood samples from 12 healthy donors (HDs), 12 atypic hyperplasia gastric mucosa (AHGM) patients and 24 gastric cancer (GC) patients were collected from Jiangsu Province Hospital (Nanjing, China), which was approved by the ethics committee of Jiangsu Province Hospital. The miRcute serum/plasma miRNA isolation kit (Tiangen Biotech Co., Ltd., Beijing, China) was used to extract the total RNA from the clinical blood samples. The 8% polyacrylamide gel electrophoresis (PAGE) was operated on a Bio-Rad electrophoretic apparatus (PowerPac Basic, BIO-RAD, USA), and the electrophoretic patterns were imaged by a GeneSys system (Syngene, UK). The fluorescence spectra were collected by a RF-5301PC fluorescence spectrophotometer (Shimadzu, Japan). The SERS spectra were measured by a confocal Raman microscope (InVia, Renishaw, England) using a 633 nm laser (1% power), a 20 × objective, 1 s exposure time and 1 time accumulation. Unless specifically stated, each presented SERS spectrum was averaged from ten measurements after subtracting the spectral baselines by the software Wire 4.3, and the error bars plotted in the figures represent the standard deviation. The Raman peak of ROX at 1503 cm^{-1} was selected as the characteristic peak for SERS analysis. In the proposed SERS sensing strategy, the SERS-active AgNRs array substrate was adopted to prepare SERS sensing chip. The substrate was patterned by a premopolydimethylsiloxane (PDMS) film with arrayed 4 × 10 wells (4 mm in diameter, 1 mm in height), and the similar photo of PDMS wells-patterned AgNRs array substrate and morphology of AgNRs array can be found in our previous works (Song et al., 2016, 2020b; Zhang et al., 2019).

2.2. Sensing mechanism of the Cas13a-bHCR biosensing strategy

Scheme 1 shows the sensing mechanism of Cas13a-bHCR based cascade signal amplification strategy for SERS sensing gastric cancer-related miR-106a, which includes a CRISPR/Cas13a system (Cas13a), branched hybridization chain reactions (bHCR), and SERS sensing chips. In the presence of target RNA (miR-106a), the miR-106a is directed by crRNA to hybridize with the spacer region (blue marked bases of crRNA in Table S1 and Scheme 1) of the Cas13a/crRNA complex, thereby to activate Cas13a (activated Cas13a, in Scheme 1) to cleave numerous recognition probes (RP) from the RNA cleavage sites (bold marked bases of RP in Table S1), resulting in the release of many reconstituted trigger (RT) fragments including 30 nucleotides (italic marked bases of RP in Table S1), i.e., one target miR-106a can activate the CRISPR/Cas13a system to generate many RTs (i.e., CRISPR/Cas13a-based signal amplification). Afterwards, three hairpin probes H1, H2, and H3 can be triggered by RT successively to undergo branched hybridization chain reactions to form branched HCR products (branched HCR, in Scheme 1, i.e., bHCR-based signal amplification). Therefore, the Cas13a-bHCR based cascade signal amplification is achieved. The following special designs of hairpin probes H1, H2, H3 and the hybridization chain reactions should be noted. H1 is labeled with a ROX molecule at its 5'-end, and its hairpin structure can be opened by the trigger of RT via the hybridization between the 20-nt bases at 3'-end of H1 (red marked in Table S1) and 5'-end of RT. H2 contains three sequence fragments, i.e., a green-marked base sequence at its 5'-end complementary to the same color-marked bases of H1 (Table S1), a base sequence complementary to red-marked bases of H1, and a toehold sequence at its 3'-end (brown marked bases of H2 in Table S1). Therefore, the H1 opened by the trigger of RT can further hybridize with H2 via the green-marked bases, and then the red-marked bases of H2 were released from the stem of H2 to hybridize with the same color marked complementary bases of another H1, which causes the primary hybridization chain reaction between H1 and H2 to generate a long DNA concatemer (HCR products) dangling many toehold sequences of H2. Moreover, H3 includes a base sequence as same as the 20-nt sequence at 5'-end of RT fragments (red marked bases at 3'-end of H3 in Table S1), which is blocked in the stem region of hairpin structure but can be opened via the hybridization with the toehold sequence of H2. In the bHCR process, the toehold sequence of H2 arranged on the primary HCR product triggers the opening of H3, and then the released 20-nt red marked bases of H3 further initiate the secondary HCR, i.e., branched HCR. The continuous HCR process results in the formation of multibranched HCR products (branched HCR, Scheme 1). Furthermore, the bHCR products are specifically captured by the capture probes (C, in Table S1) on the SERS sensing chip via the hybridization between the purple-marked complementary sequence (10 nt) at the 3'-end of the RT and the C. The SERS sensing chip is prepared by immobilizing capture probes (C) on AgNRs array by Ag–S bonds, followed by MCH blocking the C-unoccupied region to inhibit the nonspecific adsorption (SERS sensing chip, Scheme 1). As a result, significantly amplified Raman signal of ROX can be detected under the laser excitation, ascribing to the branched HCR products including numerous ROX molecules (i.e., bHCR-based signal amplification) and the excellent surface enhancement effect of AgNRs array, so that the miR-106a can be detected qualitatively and quantitatively with high sensitivity and specificity.

2.3. Characterization of the CRISPR/Cas13a system

For characterizing the effectiveness of the proposed CRISPR/Cas13a system for miR-106a detection, a special designed reporter probe (R, in Table S1) labeled with a fluorophore ROX molecule at its 5'-end and a fluorescence quencher BHQ2 molecule at its 3'-end was introduced for the promiscuous RNase activity upon target recognition of Cas13a. Specifically, 10 μL of 0.25 μM Cas13a, 10 μL of 0.25 μM crRNA, 10 μL of 2.5 μM R, and 10 μL miR-106a with a certain concentration were mixed in reaction buffer with the total reaction volume of 100 μL. The fluorescence spectra of the reaction solution were recorded immediately (0 min) and after incubation for 60 min at 37 °C, respectively. The fluorescence spectra from 597 to 700 nm were recorded under the irradiation of 587 nm light with the excitation and emission slits of 5 nm. The characteristic fluorescence peak of ROX at 604 nm was selected for data analysis. Each fluorescence spectrum shown in the manuscript was averaged from three parallel tests.

2.4. Preparation of the SERS sensing chip

The AgNRs in each PDMS well was rinsed several times with DEPC-treated water in advance. Then, 20 μL of 1 μM C was incubated with AgNRs in each well for 3 h at 37 °C to immobilize C on the AgNRs. After thoroughly washing the well with reaction buffer, 20 μL of 10 μM MCH solution was dropped in each well for 20 min to block the well in order to inhibit the nonspecific adsorption. The MCH-blocked capture probes-modified AgNRs array (i.e., SERS sensing chip) was obtained after thoroughly washing and stored at 4 °C in humid environment for future use.

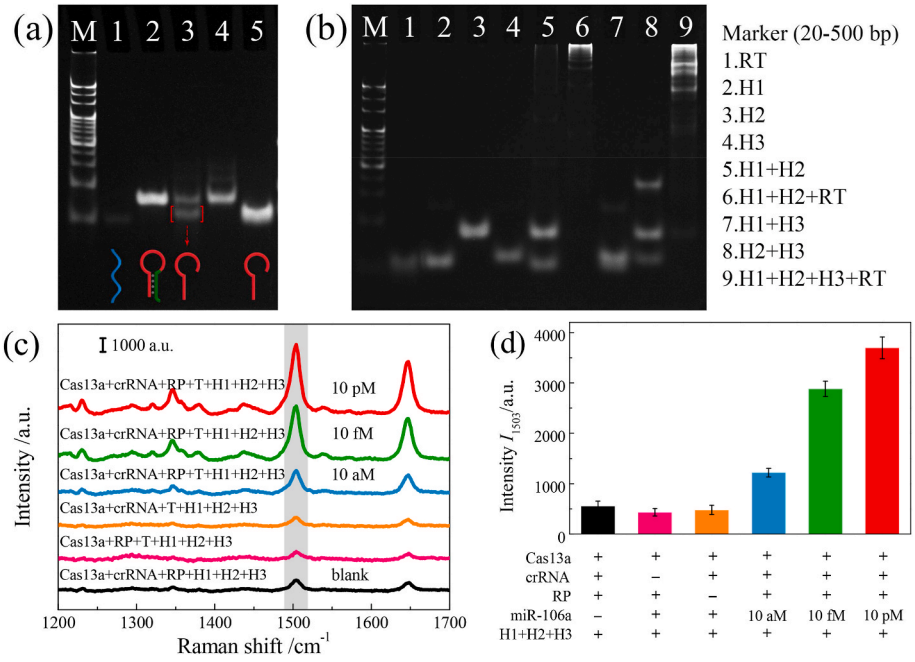

Fig. 1. Feasibility analysis of the Cas13a-bHCR based cascade signal amplification strategy for detection of miR-106a. (a) 8% PAGE gel electrophoresis analysis for CRISPR/Cas13a system. Marker (20–500 bp), lane 1: miR-106a (T), lane 2: RP, lane 3: Cas13a + crRNA + RP + T, lane 4: Cas13a + crRNA + RP, lane 5: RT. (b) 8% PAGE gel electrophoresis for bHCR amplification. Marker (20–500 bp), lane 1: RT, lane 2: H1, lane 3: H2, lane 4: H3, lane 5: H1 (1 μM) +H2 (1 μM), lane 6: H1 (1 μM) +H2 (1 μM) +RT (100 nM), lane 7: H1 (1 μM) +H3 (1 μM), lane 8: H2 (1 μM) +H3 (1 μM), lane 9: H1 (2 μM) +H2 (2 μM) +H3 (1 μM) +RT (100 nM). (c) SERS spectra obtained from the Cas13a-bHCR based cascade signal amplification strategy under the incomplete detection system in the absence of one component (i.e., T, crRNA, or RP), and the complete detection system in the presence of different concentrations of T (from 10 aM to 10 pM). (d) SERS intensities at 1503 cm^{-1} corresponding to the SERS spectra shown in (c).

2.5. SERS detection of miRNA-106a using the one-pot Cas13a-bHCR sensing strategy

The standard one-pot Cas13a-bHCR based cascade signal amplification strategy for SERS detection of miR-106a is as follows. Briefly, the one-pot strategy was conducted by mixing 2 μL of 0.25 μM Cas13a, 0.25 μM crRNA, 2.5 μM RP, 10 μM H1, 10 μM H2, 5 μM H3, and miR-106a with a certain concentration in 20 μL reaction buffer. The mixture was then dropped in each well on the SERS sensing chip and mildly shaken for 60 min at 37 °C. After thoroughly washing the well with reaction buffer and DEPC-treated water in sequence, the SERS measurements were performed after air-dry. As a control, a single CRISPR/Cas13a strategy without the bHCR was carried out in 20 μL reaction buffer including equal volume (2 μL) of 0.25 μM Cas13a, 0.25 μM crRNA, 2.5 μM RP, 10 μM H1, and miR-106a with a certain concentration, followed by the same protocol mentioned above. The concentration-dependent SERS assay was conducted by testing the miR-106a in 10% human serum with the concentrations from 10 aM to 1 nM, respectively. The specificity of the proposed SERS sensing by Cas13a-bHCR based cascade signal amplification strategy was evaluated by testing specific miR-106a (100 fM and 10 pM), 10 pM single-point mutations of target miR-106a with a base mutation at 5'-end (5'-SM), midpoint (m-SM), and 3'-end (3'-SM), 10 pM unspecific miRNAs (i.e., miR-21, miR-155, and the mixture of miR-21 and miR-155 (miR-21/155)), the mixture of 10 pM miR-21, miR-155 and miR-106a (miR-21/155/106a), and blank sample, respectively. The recovery of the SERS assay was conducted by testing miR-106a spiked in 10% human serum with the concentrations of 800 aM, 20 fM, 7 pM and 300 pM. Unless specifically stated, for each sample, three parallel experiments (n = 3) were performed.

Moreover, the practicability of the proposed SERS sensing was investigated by measuring miR-106a extracted from clinical blood samples including 12 healthy donors (HDs), 12 atypic hyperplasia gastric mucosa (AHGM) patients, and 24 gastric cancer (GC) patients. The miR-106a in the total RNAs were SERS assayed by the proposed SERS sensing strategy. Besides, the quantitative real-time polymerase chain reaction (qRT-PCR) was also performed to determine the concentration of miR-106a in the clinical blood samples. For qRT-PCR assay of the clinical samples, the total RNAs were reverse-transcribed to cDNA first. Subsequently, the PCR was conducted by the One-Step TB Green PrimeScript RT-PCR Kit II (Takara Bio Inc., Shiga, Japan), and the qRT-PCR was performed on the StepOne Plus Real-time PCR system (Applied Biosystems, USA) with the following thermocycler protocol: 95 °C for 5 min, 40 cycles of 95 °C for 15 s, 60 °C for 20 s, and 72 °C for 40 s. For each sample, three parallel tests were conducted. Similarly, the synthetic miR-106a was diluted to different concentrations of 10 fM, 100 fM, 1 pM, 10 pM and 100 pM, and then the qRT-PCR assays were performed to obtain the calibration curve of qRT-PCR assay (Kroh et al., 2010; Li, C. et al., 2022a).

3. Results and discussion

3.1. Feasibility analysis of the Cas13a-bHCR based cascade signal amplification strategy for SERS detection of miRNA-106a

The feasibility of Cas13a-bHCR based cascade signal amplification strategy for miR-106a detection was characterized by polyacrylamide gel electrophoresis (PAGE), fluorescence and SERS, and the results are shown in Fig. 1 and S1. Fig. 1a shows the electrophoresis for verifying the activity of CRISPR/Cas13a system, and the strips in lanes 1, 2 and 5 belong to the individual miR-106a, RP and RT, respectively. The mixture (Cas13a + crRNA + RP + T) in lane 3 activates the specific cleavage of RP, which lightens the strip of RP obviously and generates a new strip with the position similar to the RT in lane 5. As a control, the CRISPR/Cas13a system is inactive in the absence of T (Cas13a + crRNA + RP), which cannot cut RP. These results imply that RP can be effectively cleaved by the T-activated Cas13a to generate RT fragments. Moreover, the activity of CRISPR/Cas13a system for responding T was also characterized by the fluorescence assay by testing blank (in the absence of target) and 100 nM miR-106a by using the reporter probes (R) with quenched fluorescence. Fig. S1a shows the fluorescence spectra recorded immediately (0 min) and after the incubation for 60 min, and the corresponding fluorescence intensities were plotted in Fig. S1b. In the absence of miR-106a, there was no great change in the fluorescence signal before and after 60 min incubation. In contrast, in the presence of miR-106a, the Cas13a/crRNA complex combined with miR-106a and the CRISPR/Cas13a system was activated, and as a result significantly enhanced fluorescence signal was recorded after incubation for 60 min due to the cleavage of R (Li et al., 2021; Shan et al., 2019), which indicates that CRISPR/Cas13a system can operate well to response miR-106a. Besides, the assembly of bHCR was also be demonstrated by

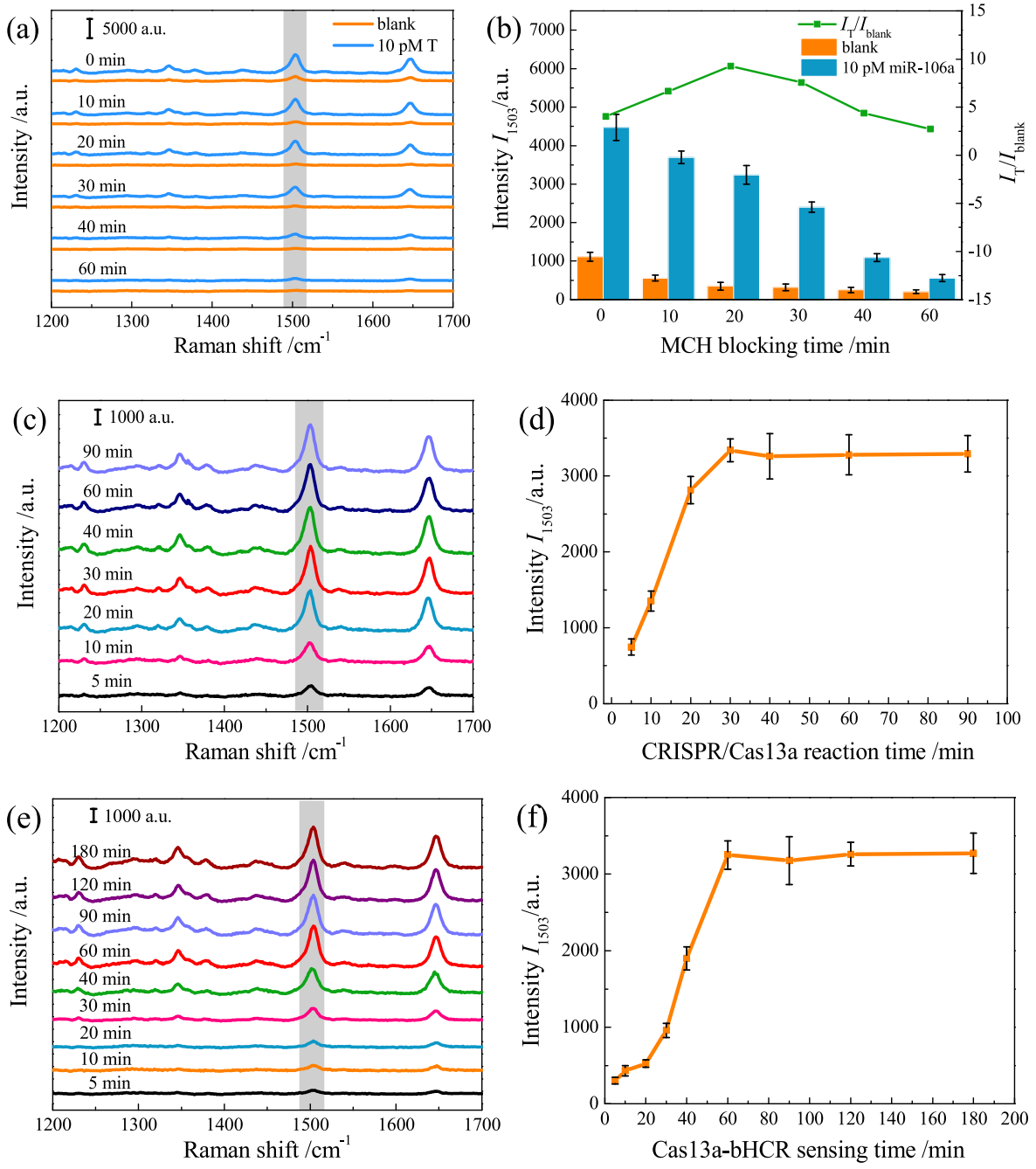

Fig. 2. Optimization of the SERS sensing strategy based on Cas13a-bHCR cascade signal amplification. (a-b) SERS spectra of the assays of 10 pM miR-106a and blank sample collected from the SERS sensing chip blocked by MCH for 0 to 60 min and the corresponding SERS intensities at 1503 cm^{-1}. (c-d) SERS spectra collected from the sensing system for the assay of 10 pM miR-106a by adjusting the CRISPR/Cas13a reaction time from 0 to 90 min, and the corresponding SERS intensities at 1503 cm^{-1}. (e-f) SERS spectra of the assay by incubating 10 pM miR-106a in Cas13a-bHCR cascade signal amplification system for 0 to 180 min, and the corresponding SERS intensities at 1503 cm^{-1}.

PAGE (Fig. 1b), and the electrophoretic stripes of RT, hairpin probes H1, H2, and H3 were shown in lanes 1 to 4, respectively. The two obvious stripes shown in lane 5 at the similar position of H1 and H2 respectively, suggesting that the H1 almost did not hybridize with H2. Once the RT was introduced into the mixture of H1 and H2, the ladder-like large stripes in lane 6 indicate the formation of DNA concatemer, i.e., the HCR products of H1 and H2, which means the efficient HCR between H1 and H2 can be successfully triggered by RT (Song et al., 2020b). The mixture of H1 and H3 (lane 7) shows little change of the stripe position relative to the ones shown in lanes 2 and 4, indicating that no hybridization occurred between the hairpin-structured H1 and H3. By mixing H2 and H3 together (lane 8), an obvious higher stripe of H2–H3 hybrids appears which means the H3 can be opened by the hybridization with the toehold sequence of H2. In lane 9, when the RT was mixed with H1, H2 and H3, the bright stripes with higher molecular weights can be observed at the gel pore, which verifies the high yield formation of the branched HCR products. Moreover, the Cas13a-bHCR based cascade signal amplification was also characterized by SERS. Fig. 1c shows the SERS spectra of the Cas13a-bHCR based cascade signal amplifications operated under the incomplete detection system in the absence of one component (i.e., T, crRNA, or RP), and the complete detection system in the presence of different concentrations of T (from 10 aM to 10 pM). The

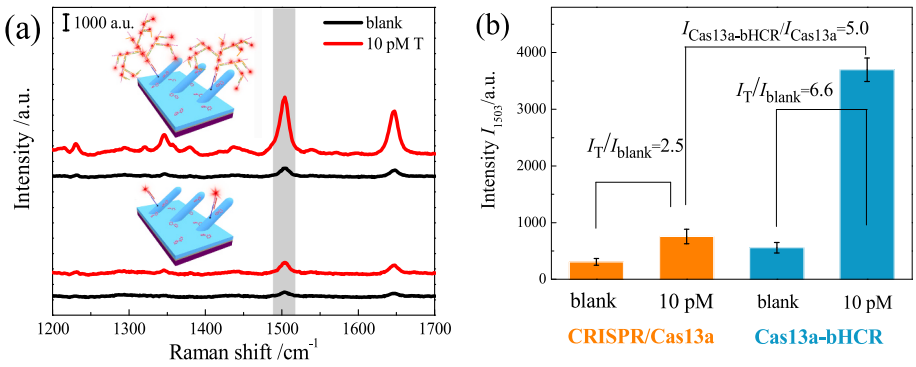

Fig. 3. Comparison of sensitivity with or without bHCR amplification based on CRISPR/Cas13a system. (a) SERS assays of 10 pM miR-106a and blank sample by following the Cas13a-bHCR based cascade signal amplification and the single CRISPR/Cas13a strategy, respectively. (b) SERS intensities at 1503 cm^{-1} corresponding to the SERS spectra shown in (a) and the calculated signal-to-noise ratios (I_T/I_{blank}).

corresponding SERS intensities at 1503 cm^{-1} are shown in Fig. 1d, in which the significant SERS signal was obtained in the presence of Cas13a/crRNA, miR-106a and RP due to the efficient cleavage of RP and the further RT-triggered branched HCR, and the SERS signal increases obviously with the increase of miR-106a concentration from 10 aM to 10 pM. In contrast, the SERS signal recorded from the incomplete detection system is similar to the one of blank. These results indicate that the CRISPR/Cas13a system can be activated by miR-106a to effectively cleave recognition probes (RP) and release numerous RTs (i.e., CRISPR/Cas13a-based signal amplification). These RTs can further trigger the branched HCR (i.e., bHCR-based signal amplification), and as a result a cascade signal amplification strategy is achieved for sensitive miR-106a detection.

3.2. Optimization of the SERS sensing strategy based on Cas13a-bHCR cascade signal amplification

To obtain the optimal sensing performance, the MCH blocking time of the SERS sensing chip, CRISPR/Cas13a reaction time and Cas13a-bHCR sensing time were optimized. In order to inhibit the nonspecific adsorption and minimize the background, the optimal MCH blocking time was investigated by blocking the AgNRs in the wells by 20 μL of 10 μM MCH for 0 to 60 min, followed by SERS detecting the blank control and 10 pM miR-106a. Fig. 2a shows the recorded SERS spectra and the corresponding SERS intensities at 1503 cm^{-1}, as well as the signal-to-noise ratio (I_T/I_{blank}) were plotted in Fig. 2b.

The SERS assay using the AgNRs with short blocking time shows relatively high background signal, and with the increase of blocking time, the background signal gradually decreases. The best signal-to-noise ratio (I_T/I_{blank}) was obtained from the SERS sensing chip blocked by MCH for 20 min, i.e., the optimal MCH blocking time was 20 min. In addition, as a very important parameter related to the efficiently yield of RT fragments (Cui et al., 2021; Shan et al., 2019), the optimal CRISPR/Cas13a reaction time is also investigated. The incubation time-dependent SERS assay was studied to monitoring the real-time kinetic process of liquid-phase sensing, and the sensing signal approaches a stable value or plateau can be considered as the optimal reaction time (Oishi and Saito, 2020; Yang et al., 2021). Fig. 2c shows the SERS spectra collected from the sensing system for the assay of 10 pM miR-106a by adjusting the CRISPR/Cas13a reaction time from 0 to 90 min, and the corresponding SERS intensities at 1503 cm^{-1} were plotted in Fig. 2d. The SERS signal monotonously increased until reaction for 30 min, which means that the optimal reaction time for CRISPR/Cas13a system is 30 min. The optimal detection time (i.e., Cas13a-bHCR sensing time) was investigated by incubating 10 pM miR-106a in Cas13a-bHCR cascade signal amplification system for 0 to 180 min, and the recorded SERS intensities reach a plateau after 60 min (Fig. 2e and f), i.e., the optimal Cas13a-bHCR sensing time is 60 min, which indicates that the Cas13a-bHCR cascade signal amplification strategy is a fast way for nucleic acid testing comparing to the conventional PCR detection for 2–4 h (Klein, 2002). Therefore, the assay conducted by a one-pot strategy by mixing sufficient reactants together may ensure the high diffusion of biomolecules to efficiently bind the target miRNAs at low concentrations (Lubken et al., 2021), and allow the multiple reactions to occur simultaneously or in a closely-related cascade so that to effectively shorten the assay time and to avoid the analyte loss caused by multi-step operation as much as possible (Chen et al., 2020; Woo et al., 2020).

3.3. Excellent performance of the Cas13a-bHCR based cascade signal amplification strategy

Fig. 3 shows the result of the SERS assays of miR-106a by following the Cas13a-bHCR based cascade signal amplification and the single CRISPR/Cas13a strategy. Fig. 3a shows the SERS spectra obtained by testing 10 pM miR-106a and the corresponding blank sample, and the SERS intensities at 1503 cm^{-1} were plotted in Fig. 3b. The SERS intensity detected by the Cas13a-bHCR based cascade signal amplification is about 5.0 times stronger than the one by single CRISPR/Cas13a strategy. In addition, the signal-to-noise ratio (I_T/I_{blank}) of the Cas13a-bHCR based cascade signal amplification strategy (I_T/I_{blank} = 6.6) is significantly improved relative to the one of single CRISPR/Cas13a strategy (I_T/I_{blank} = 2.5), which indicates that the Cas13a-bHCR based cascade signal amplification strategy has significant enhanced sensitivity of nucleic acids detection with respect to the single CRISPR/Cas13a strategy.

Fig. 4a shows the SERS assays of miR-106a in 10% human serum with the concentrations from 10 aM to 1 nM, respectively. According to concentration-dependent SERS intensity plotted in Fig. 4b, the SERS signal increases monotonically and a good linear calibration curve between the SERS intensity (I_{1503}) and the logarithm of concentrations of miR-106a ($C_{miR\text{-}106a}$) is fitted (10 aM to 1 nM), i.e., $I_{1503} = 422 \times \mathrm{Log}C_{miR\text{-}106a} + 7744$ ($R^2 = 0.993$). The limit of detection (LOD, defining as the SERS intensity of three times as large as the standard deviation of blank (Fan et al., 2021; Song et al., 2020a)) of the Cas13a-bHCR based cascade signal amplification strategy for detecting miR-106a in 10% human serum is calculated to be 8.55 aM (i.e., 5.15×10^3 copies/mL), which is much more sensitive than other reported methods for miRNA detection (Tables S2 and S3).

3.4. Specificity, uniformity and repeatability

Fig. 4c and d show the SERS spectra of specificity characterization results, and the corresponding SERS intensities at 1503 cm^{-1}, respectively. The SERS signal of specific detection (i.e., 100 fM, 10 pM miR-106a, or 10 pM miR-106a in the mixture of miR-21, miR-155 and

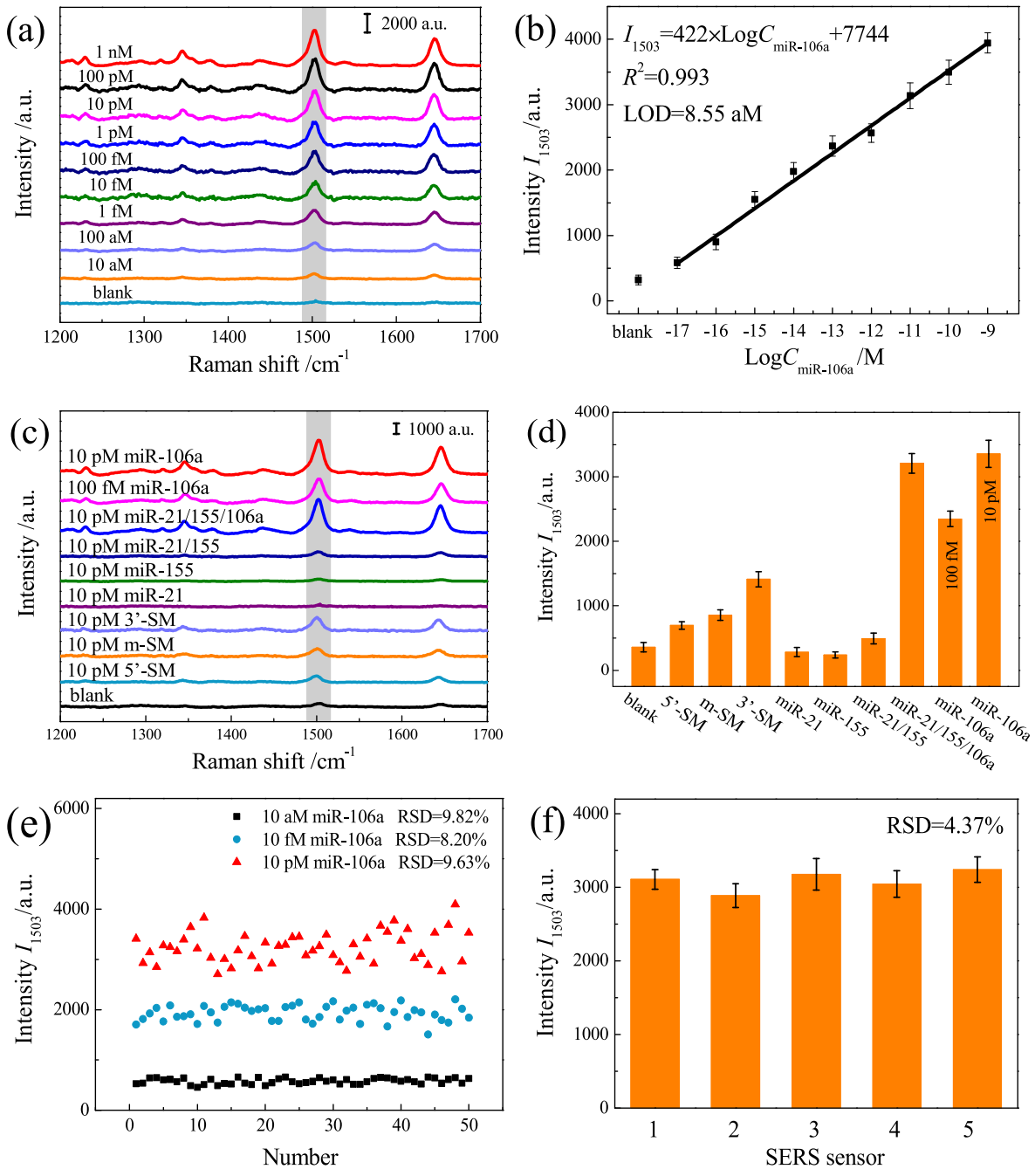

Fig. 4. Performance of the proposed SERS sensing by Cas13a-bHCR based cascade signal amplification strategy. (a) SERS assays of miR-106a in 10% human serum with the concentrations from 10 aM to 1 nM, respectively. (b) Linear plot of the concentration-dependent SERS intensity I_{1503}. (c) SERS spectra of specificity characterization, i.e., assays of 100 fM and 10 pM specific miR-106a, 10 pM unspecific samples (i.e., miR-21, miR-155, and the mixture of miR-21 and miR-155 (miR-21/155)), the mixture of 10 pM miR-21, miR-155 and miR-106a (miR-21/155/106a), the single-point mutations of miR-106a with the base mutation at 5'-end (5'-SM), midpoint (m-SM) and 3'-end (3'-SM), and the blank sample, respectively. (d) Plot of the SERS intensities at 1503 cm^{-1} corresponding to the SERS spectra shown in (c). (e) Plot of SERS intensities at 1503 cm^{-1} collected from 50 random spots on the AgNRs array for testing 10 aM, 10 fM, and 10 pM miR-106a, respectively. (f) SERS intensities at 1503 cm^{-1} obtained from 5 batches of SERS sensing chip for testing 10 pM miR-106a.

miR-106a (miR-21/155/106a)) can be distinguished apparently from the unspecific assays of miR-21, miR-155, or the mixture of miR-21 and miR-155 (miR-21/155) with the signal similar to the blank sample. Besides, even the 10 pM single-point mutations of miR-106a with a base mutation at 5'-end (5'-SM), midpoint (m-SM) or 3'-end (3'-SM) also can be significantly distinguished from the specific detections. These data indicate that the interfering miRNAs cannot trigger the operation of the Cas13a-bHCR based cascade signal amplification, and the proposed strategy has good specificity to distinguish the target miR-106a from the single-point mutations, ascribing to the single-base mismatch specificity of CRISPR/Cas13a system (Gootenberg et al., 2017; Zhang and You, 2020). Moreover, the SERS signals collected from the 50 random points on the AgNRs arrays after the assays of miR-106a with different concentrations (i.e., 10 aM, 10 fM, and 10 pM miR-106a, respectively) and from 5 batches of SERS sensing chips for testing 10 pM miR-106a show small relative standard deviations (RSD) of ≤9.82% (Fig. 4e) and 4.37% (Fig. 4f), respectively, which indicate that the proposed SERS assay has good uniformity and repeatability for achieving reliable detection of

Table 1
Recovery of the proposed SERS sensing strategy for sensing target miR-106a in 10% human serum.

Sample number	Added	Found	Recovery	RSD
1	800 aM	743.13 aM	92.89%	7.40%
2	20 fM	18.99 fM	94.95%	8.15%
3	7 pM	6.92 pM	98.86%	5.68%
4	300 pM	304.13 pM	101.4%	6.33%

disease-related nucleic acids.

3.5. Recovery of the SERS assay

The applicability of the SERS sensing strategy has been validated by testing miR-106a spiked in 10% human serum with the concentrations of 800 aM, 20 fM, 7 pM and 300 pM. The found concentrations by the SERS detection are listed in Table 1, and the recovery rates are ranged from 92.89% to 101.4% with the RSD≤8.15%, which indicates that the proposed SERS sensing strategy has good repeatability and reliability, suggesting a great potential for clinical applications.

3.6. Clinical sample assay

The practicability of the Cas13a-bHCR based SERS sensing strategy was investigated by quantifying miR-106a extracted from clinical blood samples, including 12 healthy donors (HDs), 12 atypic hyperplasia gastric mucosa (AHGM) patients, and 24 gastric cancer (GC) patients. Fig. S2a shows the SERS spectra of the miR-106a assays, and the corresponding SERS intensities at 1503 cm^{-1} are plotted in Fig. S2b. The results in Fig. 5a clearly show that the proposed Cas13a-bHCR based SERS sensing strategy can distinguish gastric cancer (GC) patients from the atypic hyperplasia gastric mucosa (AHGM) patients and healthy donors (HDs). The expression levels of miR-106a in the different clinical samples were calculated according to the linear calibration curve in Fig. 4b. Meanwhile, the qRT-PCR was used as the gold standard to determine the expression of miR-106a in clinical samples. According to the linear calibration curve between the threshold cycle (C_T) and the logarithm of miR-106a concentration ($C_{miR\text{-}106a}$) from 10 fM to 100 pM (Fig. S3), i.e., C_T = -2.54 × Log$C_{miR\text{-}106a}$ - 0.30 (R^2 = 0.998), the miR-106a in the clinical samples were quantified. As shown in Fig. 5b, the expression levels of miR-106a obtained by SERS assays were higher in blood of GC patients than those of HDs and AHGM patients ($P < 0.01$), which are in good agreement with those of the qRT-PCR with a high consistency (R^2 = 0.967) as shown in Fig. 5c. Therefore, the proposed Cas13a-bHCR based SERS sensing strategy validates the utility of miR-106a as a biomarker for the diagnosis of gastric cancer (Tsujiura et al., 2010; Xiao et al., 2009). The detailed information of the clinical diagnosis and the miR-106a expression levels tested by qRT-PCR and SERS sensing are shown in Table S4. Moreover, the area under the curve (AUC) of SERS sensing presented in the receiver operating characteristic (ROC) curve in Fig. 5d was superior compared to that qRT-PCR assay (AUCs are 0.996 and 0.979, respectively), which indicates that the proposed SERS sensing strategy holds a great potential for applications in the clinical diagnosis of gastric cancer.

4. Conclusions

In this work, a novel cascade signal amplification strategy which includes a CRISPR/Cas13a system, branched hybridization chain reactions, and SERS sensing chips was proposed for ultra-highly sensitive and specific SERS detection of disease-related nucleic acids. The sensing mechanism and feasibility of the Cas13a-bHCR based cascade signal amplification strategy were investigated and confirmed by PAGE, fluorescence and SERS. The SERS detection was then optimized and the optimal MCH blocking time of 20 min and CRISPR/Cas13a reaction time of 30 min were obtained. The SERS assays of gastric cancer-related miR-106a based on the one-pot cascade signal amplification of Cas13a-bHCR can be achieved within 60 min and output enhanced SERS signal which is about 5.0 times that of the single CRISPR/Cas13a strategy, which means a significant improved sensitivity can be achieved by the cascade signal amplification strategy. The concentration-dependent SERS assay indicates that the proposed cascade signal amplification strategy possesses a wide working range from 10 aM to 1 nM and a good linear calibration curve. The limit of detection (LOD) of miR-106a in human serum is low to 8.55 aM. Besides, the Cas13a-bHCR sensing shows good specificity, uniformity and repeatability, and the good recovery rate

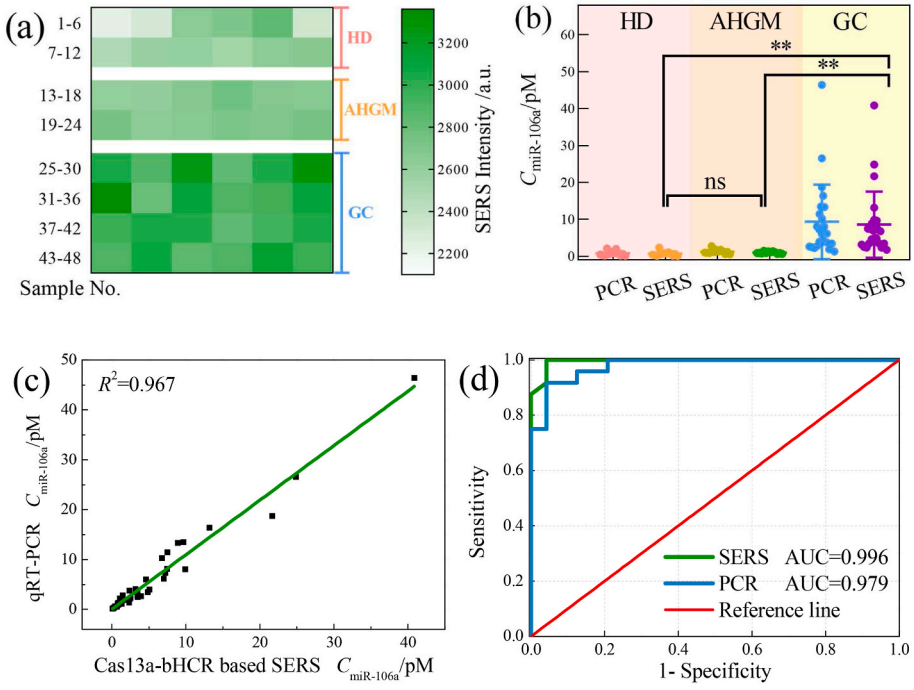

Fig. 5. Assays of miR-106a expressed in clinical blood samples collected from healthy donors (HDs) (1–12), atypic hyperplasia gastric mucosa (AHGM) patients (13–24) and gastric cancer (GC) patients (25–48) by qRT-PCR and the proposed Cas13a-bHCR based SERS sensing strategy, respectively. (a) Heatmap of miR-106a in the blood of HDs, AHGM patients and GC patients based on the SERS assay. (b) Comparison of miR-106a expression levels between qRT-PCR and the Cas13a-bHCR based SERS sensing. $^{**}P < 0.01$, ns: no significant difference ($P > 0.05$). (c) Consistency of qRT-PCR and the Cas13a-bHCR based SERS on detection of clinical samples. (d) ROC curve to evaluate the accuracy of miR-106a in clinical blood samples by qRT-PCR and SERS assay.

confirms the excellent reliability for sensing miR-106a in human serum. Moreover, the proposed Cas13a-bHCR based SERS sensing strategy can accurately quantify the miR-106a in clinical blood samples and distinguish gastric cancer (GC) patients from the atypic hyperplasia gastric mucosa (AHGM) patients and healthy donors (HDs), which can provide powerful tool for SERS detection of disease-related nucleic acids and promise brighter prospects in the field of clinical diagnosis of early disease.

CRediT authorship contribution statement

Jingjing Zhang: Methodology, Investigation, Formal analysis, Writing – original draft. **Chunyuan Song:** Conceptualization, Formal analysis, Writing – review & editing, Supervision. **Yunfeng Zhu:** Methodology, Formal analysis. **Hongyu Gan:** Methodology, Investigation. **Xinyue Fang:** Investigation, Formal analysis. **Qian Peng:** Methodology, Investigation. **Jingrong Xiong:** Formal analysis. **Chen Dong:** Methodology, Data curation. **Caiqin Han:** Resources, Validation, Writing – review & editing. **Lianhui Wang:** Project administration, Supervision, Funding acquisition.

Declaration of competing interest

The authors declare that they have no known competing financial interests or personal relationships that could have appeared to influence the work reported in this paper.

Data availability

Data will be made available on request.

Acknowledgements

This work was financially supported by the National Key Research and Development Program of China (2017YFA0205300), National Natural Science Foundation of China (61871236, 62235008, 61971207), State Key Laboratory of Applied Optics (SKLAO2022001A08), State Key Laboratory of Organic Electronics and Information Displays, and Qinglan Project of Jiangsu Province of China.

Appendix A. Supplementary data

Supplementary data to this article can be found online at https://doi.org/10.1016/j.bios.2022.114836.

References

Abell, J.L., Garren, J.M., Zhao, Y., 2011. Appl. Spectrosc. 65 (7), 734–740.
Alvarez-Puebla, R.A., Pazos-Perez, N., Guerrini, L., 2018. Appl. Mater. Today 13, 1–14.
Ang, Y.S., Yung, L.Y., 2016. Chem. Commun. 52 (22), 4219–4222.
Bienko, M., Crosetto, N., Teytelman, L., Klemm, S., Itzkovitz, S., van Oudenaarden, A., 2013. Nat. Methods 10 (2), 122–124.
Chen, J., Fan, T., Chen, Y., Ye, L., Zhang, C., Liu, F., Qin, Y., Tan, Y., Jiang, Y., 2020. Biosens. Bioelectron. 169, 112631.
Cheng, X.X., Yan, Y.R., Chen, X.P., Duan, J.X., Zhang, D.C., Yang, T.T., Gou, X.L., Zhao, M., Ding, S.J., Cheng, W., 2021. Sensor. Actuat. B-Chem. 331, 129458.
Choi, J.H., Shin, M., Yang, L., Conley, B., Yoon, J., Lee, S.N., Lee, K.B., Choi, J.W., 2021. ACS Nano 15 (8), 13475–13485.
Cui, Y., Fan, S., Yuan, Z., Song, M., Hu, J., Qian, D., Zhen, D., Li, J., Zhu, B., 2021. Talanta 224, 121878.
Driskell, J.D., Shanmukh, S., Liu, Y., Chaney, S.B., Tang, X.J., Zhao, Y.P., Dluhy, R.A., 2008. J. Mater. Chem. B 112 (4), 895–901.
East-Seletsky, A., O' Connell, M.R., Knight, S.C., Burstein, D., Cate, J.H., Tjian, R., Doudna, J.A., 2016. Nature 538 (7624), 270–273.
Fan, Z., Yao, B., Ding, Y., Zhao, J., Xie, M., Zhang, K., 2021. Biosens. Bioelectron. 178, 113015.
Gao, Y., Chen, Y., Shang, J., Yu, S., He, S., Cui, R., Wang, F., 2022. ACS Appl. Mater. Interfaces 14 (4), 5080–5089.
Gootenberg, J.S., Abudayyeh, O.O., Lee, J.W., Essletzbichler, P., Dy, A.J., Joung, J., Verdine, V., Donghia, N., Daringer, N.M., Freije, C.A., Myhrvold, C., Bhattacharyya, R.P., Livny, J., Regev, A., Koonin, E.V., Hung, D.T., Sabeti, P.C., Collins, J.J., Zhang, F., 2017. Science 356 (6336), 438–442.
Huang, D., Li, X., Shen, B., Li, J., Ding, X., Zhou, X., Guo, B., Cheng, W., Ding, S., 2018. Sensor. Actuat. B-Chem. 273, 393–399.
Hui, X., Yang, C., Li, D., He, X., Huang, H., Zhou, H., Chen, M., Lee, C., Mu, X., 2021. Adv. Sci. 8 (16), e2100583.
Jiao, J., Duan, C., Xue, L., Liu, Y., Sun, W., Xiang, Y., 2020. Biosens. Bioelectron. 167, 112479.
Kellner, M.J., Koob, J.G., Gootenberg, J.S., Abudayyeh, O.O., Zhang, F., 2019. Nat. Protoc. 14 (10), 2986–3012.
Klein, D., 2002. Trends Mol. Med. 8 (6), 257–260.
Kong, M., Li, Z., Wu, J., Hu, J., Sheng, Y., Wu, D., Lin, Y., Li, M., Wang, X., Wang, S., 2019. Talanta 205, 120155.
Kroh, E.M., Parkin, R.K., Mitchell, P.S., Tewari, M., 2010. Methods 50 (4), 298–301.
Li, C.C., Hu, J., Zou, X., Luo, X., Zhang, C.Y., 2022a. Anal. Chem. 94 (3), 1882–1889.
Li, H., Yang, J., Wu, G., Weng, Z., Song, Y., Zhang, Y., Vanegas, J.A., Avery, L., Gao, Z., Sun, H., Chen, Y., Dieckhaus, K.D., Gao, X., Zhang, Y., 2022b. Angew. Chem. Int. Ed. 61 (32), e202203826.
Li, S., Li, P., Ge, M., Wang, H., Cheng, Y., Li, G., Huang, Q., He, H., Cao, C., Lin, D., Yang, L., 2020. Nucleic Acids Res. 48 (5), 2220–2231.
Li, Y., Teng, X., Zhang, K., Deng, R., Li, J., 2019. Anal. Chem. 91 (6), 3989–3996.
Li, Z., Zhao, W., Ma, S., Li, Z., Yao, Y., Fei, T., 2021. Biosens. Bioelectron. 192, 113493.
Liu, L., Li, X., Ma, J., Li, Z., You, L., Wang, J., Wang, M., Zhang, X., Wang, Y., 2017. Cell 170 (4), 714–726 e710.
Liu, R., Zhang, S., Zheng, T.T., Chen, Y.R., Wu, J.T., Wu, Z.S., 2020. ACS Nano 14 (8), 9572–9584.
Liu, Y.J., Chu, H.Y., Zhao, Y.P., 2010. J. Phys. Chem. C 114 (18), 8176–8183.
Lubken, R.M., Bergkamp, M.H., de Jong, A.M., Prins, M.W.J., 2021. ACS Sens. 6 (12), 4471–4481.
Markou, A., Tsaroucha, E.G., Kaklamanis, L., Fotinou, M., Georgoulias, V., Lianidou, E.S., 2008. Clin. Chem. 54 (10), 1696–1704.
Moisoiu, V., Iancu, S.D., Stefancu, A., Moisoiu, T., Pardini, B., Dragomir, M.P., Crisan, N., Avram, L., Crisan, D., Andras, I., Fodor, D., Leopold, L.F., Socaciu, C., Balint, Z., Tomuleasa, C., Elec, F., Leopold, N., 2021. Colloids Surf., B 208, 112064.
Nam, T.W., Park, Y., Jung, Y.S., Park, H.G., 2022. ACS Nano 16 (7), 11115–11123.
Nie, S., Emory, S.R., 1997. Science 275 (5303), 1102–1106.
Notomi, T., Okayama, H., Masubuchi, H., Yonekawa, T., Watanabe, K., Amino, N., Hase, T., 2000. Nucleic Acids Res. 28 (12), E63.
Oishi, M., Saito, K., 2020. ACS Nano 14 (3), 3477–3489.
Rohrman, B.A., Richards-Kortum, R.R., 2012. Lab Chip 12 (17), 3082–3088.
Shan, Y., Zhou, X., Huang, R., Xing, D., 2019. Anal. Chem. 91 (8), 5278–5285.
Smyrlaki, I., Ekman, M., Lentini, A., Rufino de Sousa, N., Papanicolaou, N., Vondracek, M., Aarum, J., Safari, H., Muradrasoli, S., Rothfuchs, A.G., Albert, J., Hogberg, B., Reinius, B., 2020. Nat. Commun. 11 (1), 4812.
Song, C., Jiang, X., Yang, Y., Zhang, J., Larson, S., Zhao, Y., Wang, L., 2020a. ACS Appl. Mater. Interfaces 12 (28), 31242–31254.
Song, C., Zhang, J., Liu, Y., Guo, X., Guo, Y., Jiang, X., Wang, L., 2020b. Sensor. Actuat. B-Chem. 325, 128970.
Song, C.Y., Yang, Y.J., Yang, B.Y., Sun, Y.Z., Zhao, Y.P., Wang, L.H., 2016. Nanoscale 8 (39), 17365–17373.
Tang, Y., Song, T., Gao, L., Yin, S., Ma, M., Tan, Y., Wu, L., Yang, Y., Wang, Y., Lin, T., Li, F., 2022. Nat. Commun. 13 (1), 4667.
Tate, J., Ward, G., 2004. Clin. Biochem. Rev. 25 (2), 105–120.
Tian, T., Shu, B., Jiang, Y., Ye, M., Liu, L., Guo, Z., Han, Z., Wang, Z., Zhou, X., 2021. ACS Nano 15 (1), 1167–1178.
Tomita, N., Mori, Y., Kanda, H., Notomi, T., 2008. Nat. Protoc. 3 (5), 877–882.
Tsujiura, M., Ichikawa, D., Komatsu, S., Shiozaki, A., Takeshita, H., Kosuga, T., Konishi, H., Morimura, R., Deguchi, K., Fujiwara, H., Okamoto, K., Otsuji, E., 2010. Br. J. Cancer 102 (7), 1174–1179.
Wang, B., Thachuk, C., Ellington, A.D., Winfree, E., Soloveichik, D., 2018. Proc. Natl. Acad. Sci. U.S.A. 115 (52). E12182-E12191.
Wang, C., Huang, C.H., Gao, Z., Shen, J., He, J., MacLachlan, A., Ma, C., Chang, Y., Yang, W., Cai, Y., Lou, Y., Dai, S., Chen, W., Li, F., Chen, P., 2021. ACS Sens. 6 (9), 3308–3319.
Wang, J., Wang, D.X., Ma, J.Y., Wang, Y.X., Kong, D.M., 2019. Chem. Sci. 10 (42), 9758–9767.
Wang, M., Zhang, R., Li, J., 2020. Biosens. Bioelectron. 165, 112430.
Wang, Y., Zheng, D., Tan, Q., Wang, M.X., Gu, L.Q., 2011. Nat. Nanotechnol. 6 (10), 668–674.
Woo, C.H., Jang, S., Shin, G., Jung, G.Y., Lee, J.W., 2020. Nat. Biomed. Eng. 4 (12), 1168–1179.
Wu, X., Tay, J.K., Goh, C.K., Chan, C., Lee, Y.H., Springs, S.L., Wang, Y., Loh, K.S., Lu, T. K., Yu, H., 2021. Biomaterials 274, 120876.
Xiao, B., Guo, J., Miao, Y., Jiang, Z., Huan, R., Zhang, Y., Li, D., Zhong, J., 2009. Clin. Chim. Acta 400 (1–2), 97–102.
Xu, J., Suo, W., Goulev, Y., Sun, L., Kerr, L., Paulsson, J., Zhang, Y., Lao, T., 2021. Small, e2104009.
Xu, Y., Wang, H., Luan, C., Fu, F., Chen, B., Liu, H., Zhao, Y., 2018. Adv. Funct. Mater. 28 (1), 1704458.
Yang, H., Weng, B., Liu, S., Kang, N., Ran, J., Deng, Z., Wang, H., Yang, C., Wang, F., 2022. Biosens. Bioelectron. 204, 114060.
Yang, Y., Liu, J., Zhou, X., 2021. Biosens. Bioelectron. 190, 113418.
Zhang, C., Zhao, Y., Xu, X., Xu, R., Li, H., Teng, X., Du, Y., Miao, Y., Lin, H.C., Han, D., 2020. Nat. Nanotechnol. 15 (8), 709–715.
Zhang, J., Miao, X., Song, C., Chen, N., Xiong, J., Gan, H., Ni, J., Zhu, Y., Cheng, K., Wang, L., 2022. Biosens. Bioelectron. 212, 114379.
Zhang, J., Yang, Y., Jiang, X., Dong, C., Song, C., Han, C., Wang, L., 2019. Biosens. Bioelectron. 141, 111402.

Zhang, J., You, Y., 2020. Cancer Biol. Med. 17 (1), 6–8.
Zhou, H., Liu, J., Xu, J.J., Zhang, S.S., Chen, H.Y., 2018. Chem. Soc. Rev. 47 (6), 1996–2019.
Zhu, K., Yang, K., Zhang, Y., Yang, Z., Qian, Z., Li, N., Li, L., Jiang, G., Wang, T., Zong, S., Wu, L., Wang, Z., Cui, Y., 2022. Small 18 (32), e2201508.
Zong, C., Xu, M., Xu, L.J., Wei, T., Ma, X., Zheng, X.S., Hu, R., Ren, B., 2018. Chem. Rev. 118 (10), 4946–4980.